AD NUMBER

ADB220035

NEW LIMITATION CHANGE

TO

Approved for public release, distribution unlimited

FROM

Distribution authorized to U.S. Gov't. agencies only; Proprietay Info.; Sep 96. Other requests shall be referred to Commande, U.S, Army Medical Research and Materiel Command, Attn: MCMR-RMI-S, Fort Detrick, Frederick, MD 21702-5012.

AUTHORITY

USAMRMC ltr, 1 Jun 2001.

AD_____

GRANT NUMBER DAMD17-94-J-4055

TITLE: Direct Digital Mammography Using Capillary Optics

PRINCIPAL INVESTIGATOR: Carolyn A. MacDonald, Ph.D.

CONTRACTING ORGANIZATION: New York State University at Albany
Albany, NY 12201-0009

REPORT DATE: September 1996

TYPE OF REPORT: Annual

PREPARED FOR: Commander
U.S. Army Medical Research and Materiel Command
Fort Detrick, Frederick, Maryland 21702-5012

REPORT DOCUMENTATION PAGE

Form Approved
OMB No. 0704-0188

1. AGENCY USE ONLY *(Leave blank)*	2. REPORT DATE	3. REPORT TYPE AND DATES COVERED
	September 1996	Annual (1 Sep 95 - 31 Aug 96)

4. TITLE AND SUBTITLE Direct Digital Mammography Using Capillary Optics

5. FUNDING NUMBERS
DAMD17-94-J-4055

6. AUTHOR(S)
Carolyn A. MacDonald, Ph.D.

7. PERFORMING ORGANIZATION NAME(S) AND ADDRESS(ES)
New York State University at Albany
Albany, NY 12201-0009

8. PERFORMING ORGANIZATION REPORT NUMBER

9. SPONSORING/MONITORING AGENCY NAME(S) AND ADDRESS(ES)
U.S. Army Medical Research and Materiel Command
Fort Detrick
Frederick, Maryland 21702-5012

10. SPONSORING/MONITORING AGENCY REPORT NUMBER

11. SUPPLEMENTARY NOTES

12a. DISTRIBUTION / AVAILABILITY STATEMENT
Distribution authorized to U.S. Government agencies only; Proprietary Information, Sep 96. Other requests for this document shall be referred to Comander, U.S. Army Medical Research and Materiel Command, ATTN: MCMR-RMI-S, Fort Detrick, Frederick, MD 21702-5012

12b. DISTRIBUTION CODE

13. ABSTRACT *(Maximum 200*

The overall objective of this proposal is to develop a mammographic system with extremely high scatter rejection and dynamic range, good resolution and low patient dose. This will be accomplished by developing a direct x-ray detector interfaced with a capillary x-ray optic in an appropriately designed mammographic system.

Measurements have been performed of transmission and absorbence of single capillaries. Preliminary measurements have been performed of pre-prototype optics. These measurements indicate that capillary x-ray optics should be suitable for enhancing contrast and performing beam shaping for matching with digital detectors. Simulation work on a collimating optic has shown good agreement with data and is progressing, which has allowed some design decisions for a suitable optic to be made. A prototype linear detector array has been constructed, along with readout electronics. A single pixel detector has been characterized.

14. SUBJECT TERMS	15. NUMBER OF PAGES
Breast Cancer, Mammography, Digital Mammography, Early Detection, Capillary X-ray Optics	20
	16. PRICE CODE

17. SECURITY CLASSIFICATION OF REPORT	18. SECURITY CLASSIFICATION OF THIS PAGE	19. SECURITY CLASSIFICATION OF ABSTRACT	20. LIMITATION OF ABSTRACT
Unclassified	Unclassified	Unclassified	Limited

FOREWORD

Opinions, interpretations, conclusions and recommendations are those of the author and are not necessarily endorsed by the US Army.

CAM Where copyrighted material is quoted, permission has been obtained to use such material.

CAM Where material from documents designated for limited distribution is quoted, permission has been obtained to use the material.

CAM Citations of commercial organizations and trade names in this report do not constitute an official Department of Army endorsement or approval of the products or services of these organizations.

____ In conducting research using animals, the investigator(s) adhered to the "Guide for the Care and Use of Laboratory Animals," prepared by the Committee on Care and Use of Laboratory Animals of the Institute of Laboratory Resources, National Research Council (NIH Publication No. 86-23, Revised 1985).

____ For the protection of human subjects, the investigator(s) adhered to policies of applicable Federal Law 45 CFR 46.

____ In conducting research utilizing recombinant DNA technology, the investigator(s) adhered to current guidelines promulgated by the National Institutes of Health.

____ In the conduct of research utilizing recombinant DNA, the investigator(s) adhered to the NIH Guidelines for Research Involving Recombinant DNA Molecules.

____ In the conduct of research involving hazardous organisms, the investigator(s) adhered to the CDC-NIH Guide for Biosafety in Microbiological and Biomedical Laboratories.

Carolyn A MacDonald 9/27/96

PI - Signature Date

Table of Contents

Introduction

Nature of the Problem

While it is hoped that molecular detection and intervention will one day provide a more effective treatment modality, currently, in the words of the Report to the U.S. Army Medical Research and Development Command on the Strategies for Managing the Breast Cancer Research Program, "no dominant etiology for breast cancer has emerged...[this] would lessen the prospects for any quick and easy prevention strategies.... mammography is the method of choice for screening women to detect breast cancer ... mammography has proven to be the most effective means of reducing breast cancer morbidity and mortality."

The primary theoretical limitations of mammography are the system resolution, which determines the minimum size of the detectable malignancy, and the need to expose the patient to ionizing radiation. Using innovative new technology to improve system resolution and reduce required dose will increase the effectiveness of this proven screening modality, with a direct and immediate impact on mortality. In addition, this direct digital system can avail itself of the advantages of digital processing, including improved image contrast and resolution at reduced radiation dose.[1] In practice, mammographic imaging is often limited by quality assurance issues, which can also be favorably addressed by digital processing.

Purpose

The overall objective of this proposal is to develop a mammographic system with extremely high scatter rejection and dynamic range, good resolution and low patient dose. This will be accomplished by developing a direct x-ray detector interfaced with a capillary x-ray optic in an appropriately designed mammographic system.

Kumakhov capillary x-ray optics, invented in the mid-eighties, provide an innovative new way to control x-ray beams. Such optics will provide extremely efficient scatter rejection, while allowing beam demagnification and shaping to match with the newly developing high efficiency direct x-ray detectors. These detectors owe their high efficiency and resolution to the direct detection of x-ray photons without requiring phosphors for the conversion to visible light. An integrated system of optics and detectors will be developed in a highly collaborative effort involving recognized leaders in the fields of capillary optics, x-ray detectors, digital radiology, and mammography. Testing will be performed on each of the elements independently, and as an integrated unit in a mammographic system.

Background

Benefits of Digital Mammography

Conventional film/screen mammography suffers from limited dynamic range and film granularity which can reduce the sensitivity of detection of microcalcifications. Digital detection can provide high dynamic range, which in addition to improving contrast, greatly increases the tolerance of the final image to under- or over-exposure. Digital images can be enhanced and are amenable to computer aided diagnosis. Spectral information can be included if it is available. Finally, digital images can be quickly transported for skilled consultation.

Capillary Optics

Kumakhov capillary optics are bundles of hollow glass capillary tubes with inner diameters as small as a few microns. X rays incident on the interior of the glass tubes at small angles can be guided down the tubes by total external reflection. The capillaries guide x rays in a manner analogous to the way fiber optics guide light. Arrays of curved tapered capillaries can be used to focus, collimate and filter x-ray radiation.[2,3,4,5,6] Such arrays can be manufactured by stringing hollow glass polycapillaries through metal grids, or manufactured without grids as a monolithic optic.

The critical angle for total external reflection of x rays by glass polycapillaries is

$$\theta_c = \frac{\omega_p}{\omega},$$

where ω_p is the plasma frequency of the glass, about 30 eV, and ω is the photon frequency. The critical angle is 1.5 milliradians at 20 keV. The x rays can be transmitted in a curved tube so long as the tube is small enough and bent gently enough that the angles of incidence are kept less than the critical angle. For a given radius of curvature, this requires increasingly small diameter tubes as the x-ray energy is raised. In order to avoid the mechanical limitations of such small tube sizes, polycapillary fibers are employed with channel sizes (typically 1-30 μm) much smaller than the outer diameter (300-1000 μm).

The use of Kumakhov capillary optics in place of more conventional scatter reduction grids in a mammographic system has significant potential to provide improved resolution, increased contrast enhancement, and reduced dose in mammographic imaging. The optics can also be used to mate the radiographic image with a digital detector by appropriate choice of demagnification and separation to discrete chips. In addition, a pre-patient optic could be employed to increase the available intensity in a fan beam relative to simple slot collimation.

Digital X-Ray Detection

In almost all radiological systems, detection of x rays is performed by the use of a "phosphor" screen which converts absorbed x rays into visible light photons. The visible light is then recorded on an analog medium, such as film, or detected by a digital detector. The phosphor screen is used because most detectors, including film, are not particularly sensitive to x rays. The use of a screen-film combination reduces radiation requirement compared to direct exposure film by a factor of 50-100.[7] This increase in

sensitivity occurs at the expense of resolution. The modulation transfer function of a good film-screen combination drops to less than 0.1 at a frequency of 15 lp/mm.[7] The choice of screen thickness is a trade-off between detected quantum efficiency, which improves with increasing thickness, and resolution, which is degraded by light blur in a thick screen.[8]

Efficient direct x-ray detection virtually eliminates the tradeoff between spatial resolution and sensitivity because of the elimination of the phosphor screen. Direct x-ray detectors can provide resolution of 20 lp/mm or better with nearly 100% Detector Quantum Efficiency (DQE).

An especially promising direct x-ray detector is the cadmium zinc telluride (CZT) semiconductor detector recently developed by Digirad, formerly Aurora Technologies. The DQE of a .5 mm thick CZT detector is essentially unity at 20 keV, while the resolution is to first order independent of thickness. CZT detectors are similar in many respects to cadmium telluride (CdTe) detectors which have been available commercially for many years. The replacement of a fraction of the Cd with Zn causes a wider bandgap and results in a resistivity increase of two orders of magnitude. This high resistivity is an important factor because it reduces leakage current, a significant source of performance degrading noise. Leakage current noise generally limits the use of CdTe detectors by requiring longer integration times and larger pixel sizes.

Body: Methods and Results

To provide a framework for assessing the results of the first two years of the project, the original statement of work for the full four year project is reproduced here.

Proposed Statement of Work

I. Development of Capillary Optic Mammographic System: Months 1-36

I.A. Single Capillary Measurements: Months 1-6

I.B. Simulation of Design Strategies: Months 6-18

I.C. Assembly and Testing of Prototype Optic: Months 18-24

I.D. Design of Final Mammographic Optics and Detector Unit: Months 20-28

I.E. Assembly and Testing of Final Optic: Months 28-36

II. Development of Digital Detector: Months 1-24

II.A. Fabricate CZT Linear Detector Arrays: Months 1-24

II.B. Develop Interconnect Methodology (Wire Bonding): Months 2-8

II.C. Assemble and Test Proof of Principle Detector/Multiplexer Hybrid : Months 2-12

II.D. Assemble Additional Hybrid Arrays: Months 12-24

III. Mammographic Measurements: Months 18-48

III.A. Measurement of Prototype System: Months 18-36

III.A.1 Design and Fabrication of Test System: Months 18-24

III.A.2. Measure Primary Transmission in a Mammographic Geometry: Months 24-30

III.A.3 Measure Transmission of Scattered Radiation: Months 24-30

III.A.4. Spectral Measurements: Months 24-30

III.A.5. Investigate Artifacts due to Capillary Structure: Months 30-36

III.A. 6. Measure Contrast Improvement and Resolution: Months 30-36

III.B. Measurement of Final Optics/Detector System: Months 28-48

III.B.1. Design and Fabrication of Measurement System: Months 28-36

III.B.2. Measure Primary Transmission in a Mammographic Geometry: Months 36-42

III.B.3. Measure Transmission of Scattered Radiation: Months 36-42

III.B.4. Spectral Measurements: Months 36-42

III.B.5. Investigate Artifacts due to Capillary Structure: Months 42-48

III.B.6. Measure Contrast Improvement and Resolution: Months 42-48

III.B.7. Evaluate Image Quality Using RMI Breast Phantom: Months 42-48

Progress to Date

Task I.A. Single Capillary Measurements

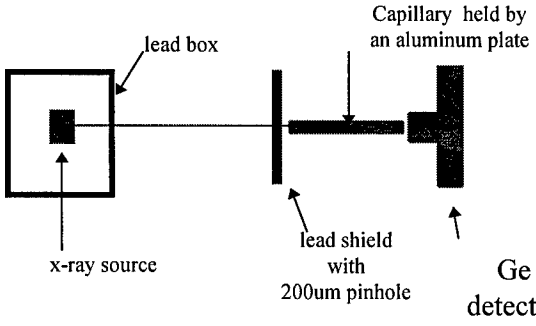

Figure 1. Experimental setup.

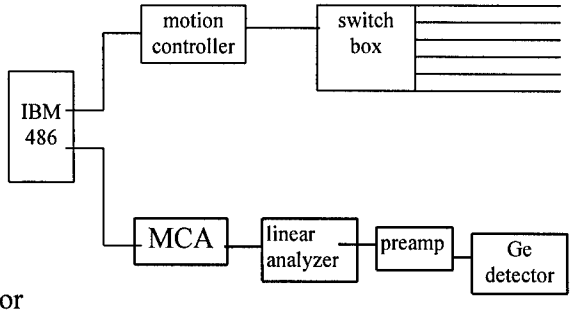

Figure 2. Electronic system

Type	Description	Outer Diameter, mm	Channel Size, μm	Area	Length, mm
A	Borosilicate	0.5	12	65%	105
B	Lead glass	0.5	12	52%	95
C	Borosilicate	0.75	22	50%	136
D	Borosilicate	4	12	55%	130
E	Borosilicate	0.3	4-5	55%	105

Table 1. Description of polycapillary fibers

Task I.A. is complete. The experimental arrangement for single capillary measurements is shown in figures 1 and 2. An optical rail affixed to an optical table carries an x-ray source, fiber platform, and x-ray detector. Each can be positioned independently in three dimensions. A collimator is placed before the fiber and any remaining x-ray leakage around the fiber is eliminated with metal powder or filings. The measured fibers are described in Table 1. The results of transmission studies as a function of photon energy are shown in Figure 3.[9 10] All of the fibers except the lead glass have transmissions at 20 keV nearly equal to their fractional open area (the fraction of the cross section of the capillary which is open space, the rest being glass walls). This transmission corresponds to the primary transmission expected for a linear capillary optic employed as an antiscatter grid.

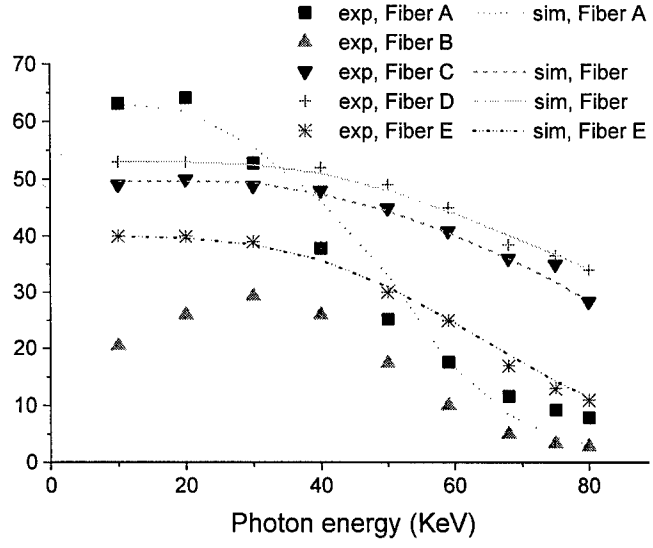

Figure 3. Measured transmission versus energy for polycapillary fibers listed in Table 1.

Measurements to determine the capacity of the glass optic to absorb scatter radiation were performed by increasing the angle to

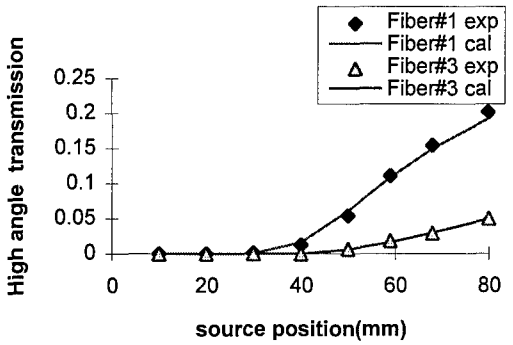

Figure 4. High angle transmission through capillary walls as a function of photon energy. Fiber#1:l=105mm Fiber#3:l=136mm

the source, relative to the fiber axis, to an angle much greater than the critical angle for the total external reflection. (Total external reflection carries the primary photons down the channel.) Results of these "high angle transmission" measurements are shown I in Figure 4. This transmission corresponds to scatter transmission for the capillary optics used as an antiscatter grid, and is less than 1% at 20 keV. The solid line is a theoretical calculation, which agrees quite well with the data.

It has been elected to perform measurements of divergence and of the transmission of bent fibers on "pre-prototype" systems which more closely resemble prototype mammographic optics than do individual single fibers. These measurements are described under Task III.A. below.

Task I.B. Simulation of Design Strategies

This task is nearing completion. To evaluate the experimental performance of capillaries, and design capillary optics, it is necessary to be able to predict theoretical behavior for complex geometries. A modeling program for single fibers based on a Monte Carlo simulation of simple geometrical optics has been developed. The computational speed is greatly enhanced by a reduction to two dimensions by projecting the trajectory onto the local fiber cross-section.[11] Reflectivities are computed from standard tables.[12] Significant recent progress has been made in understanding the effect of capillary profile error, waviness and roughness on the transmission

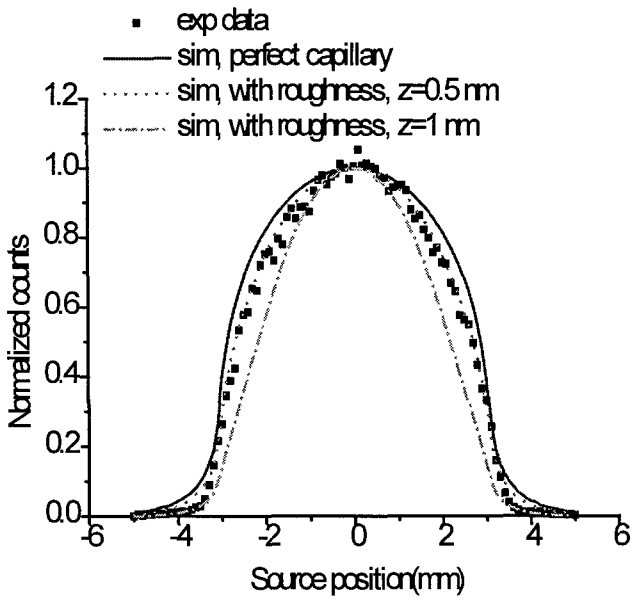

Figure 6. Simulated source scan curves of Fiber 3 at 10 keV compared with experimental data.

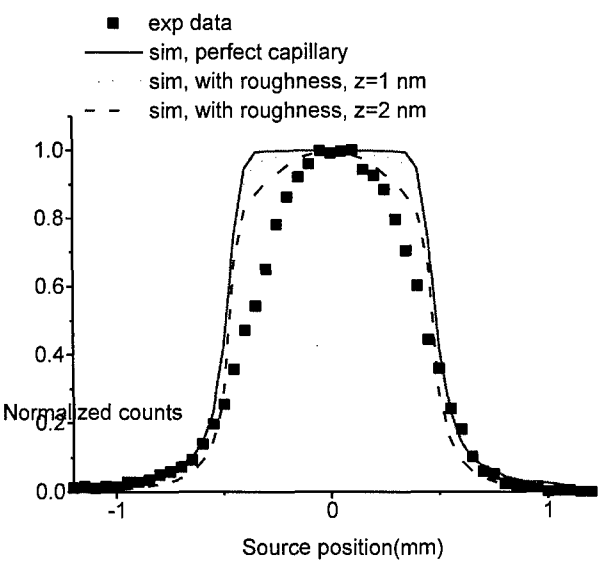

Figure 5. Simulated source scan curves at 68 keV of Fiber 3 with different roughness corrections compared with the experimental data.

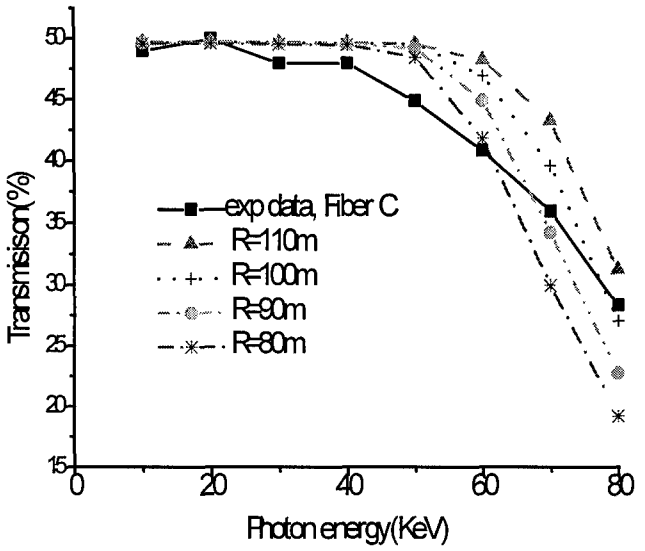

Figure 7. Transmission spectra of Fiber 3 simulated with different bending curvature alone and compared with experimental data

spectra.[13] This is extremely important in providing feedback to the manufacturing process.

In Figure 5, simulations with or without roughness corrections are compared with the experimental data. In these measurements the source is scanned transverse to the fiber axis. The simulation with a roughness height of 0.5 nm fits the experimental data quite well. It is definitely over-corrected when the roughness is 1.0 nm. The same simulations are also carried out at 68 keV, where the width of the curve is narrower than that at 10 keV because of the smaller critical angle. Photons also experience fewer bounces on average. As shown in Figure 6, simulations with roughnesses as large as 1.0 and 2.0 nm still could not fit the data. Knowing that 1.0 or 2.0 nm roughness is definitely too large at 10 keV, we can determine that the roughness correction by itself is not sufficient at high energy to reproduce source scan measurements. Other effects need to be considered. These are bending and waviness.

A slight bending of the capillary can dramatically reduce the transmission of high energy photons because of the small critical angle. A comparison between experimental data and simulations with different bending is shown in Figure 7. The figure shows that the simulations with bending alone do not fit the experimental data well, which indicates that bending is not the only factor which causes the high energy transmission to drop. However, from Figure 7, we can see that the range of the bending radius must be larger than 100m to give the observed transmission at the highest energy(80KeV).

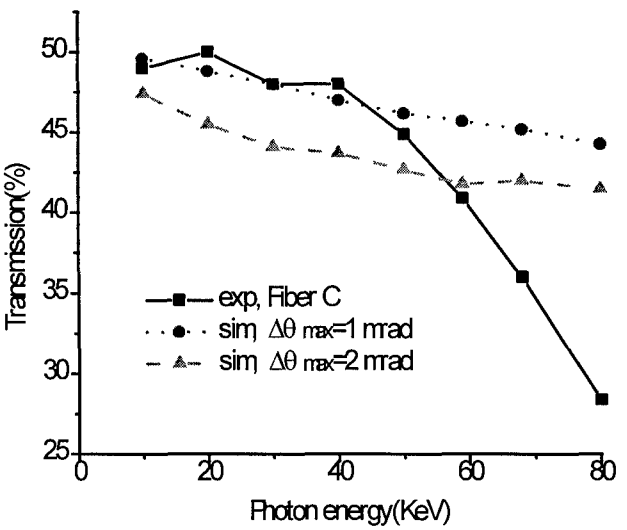

Figure 8. Simulations of transmission spectra with waviness only compared with the experimental data.

Capillary surface oscillations with wavelengths shorter than the capillary length and longer than the wavelength of the roughness are called waviness. The detailed shape of waviness is unknown. Its average effect can be considered as a random tilt of the glass wall, so that the grazing angle of the photon is changed by a random amount, $\delta\theta$, after every bounce. $\delta\theta$ is a random number between $-\Delta\theta_{max}$ and $\Delta\theta_{max}$ if $\theta \geq \Delta\theta_{max}$. The maximum random tilt angle $\Delta\theta_{max}$ is an adjustable parameter which depends on the waviness of the capillary. To keep θ' positive, $\delta\theta$ is taken to be a random number between $-\theta$ and $\Delta\theta_{max}$ when $\theta < \Delta\theta_{max}$. Since a photon with an incident angle smaller than $\Delta\theta_{max}$ has a larger chance to experience an angle increase than an angle decrease, this is physically reasonable. In Figure 8, simulations with waviness corrections with $\Delta\theta_{max}$ set at 1 mrad and 2 mrad, which is comparable to the critical angle, are compared with the experimental data. This figure shows that simulations with waviness alone do not fit the experimental data. This is because the waviness correction changes the reflected angle, not the profile. In fact the capillary is still considered to be straight, so those photons which have few reflections will not be significantly effected by waviness.

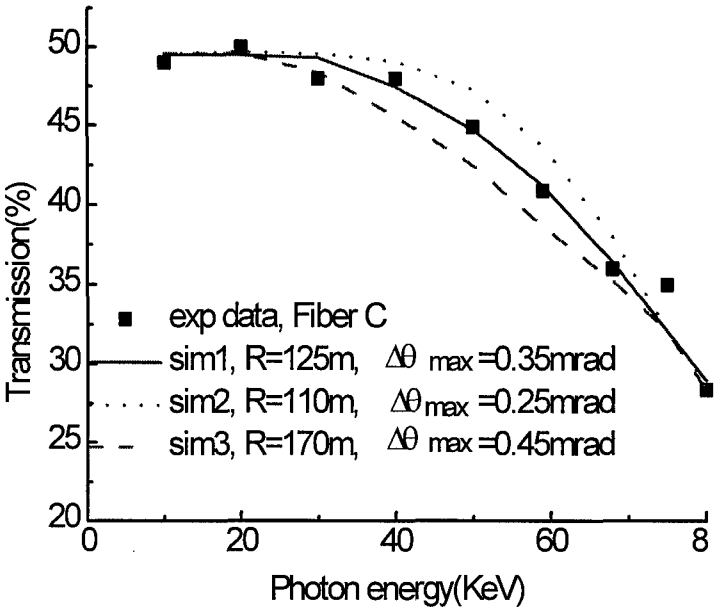

Figure 9. Simulated transmission spectra with different bending and waviness compared with the experimental data in search for the best fitting of Fiber C.

Finally the waviness and bending are combined by increasing the bending radius R, roughly determined in Figure 7, and adding a waviness parameter, $\Delta\theta$max. Several trials are shown in Figure 9. Sim2 has too much bending and not enough waviness; sim3 has too much waviness and not enough bending; sim1 is the best fit. Roughness is also included in those simulations. The source scan simulation with the three fixed parameters are plotted along with the experimental data in Figure 9 for four more photon energies. They all fit fairly well.

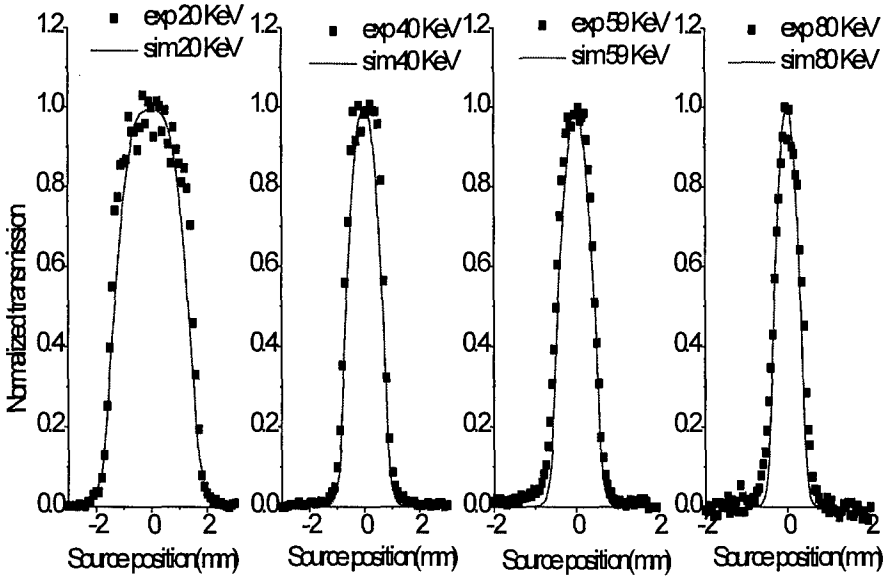

Figure 10. Simulated source scan curves compared with experimental data at four different photon energies. Parameters are: R = 125 m, Δθmax= 0.35 mrad, roughness height=0.5 nm.

A similar procedure was used to determine the simulation parameters for the remaining fibers. The results are shown in Figure 3.

Examining Figure 3 again, the channel transmission for fiber A shows a rapid drop for energies above 30 keV. This capillary is thin (500 μm in diameter) and flexible, and therefore difficult to keep straight in the measurement apparatus. Any slight bending is more significant at high energies, where the critical angles are smaller. Transmission for fiber C and fiber D are nearly flat up to 60 keV. As noted in table 1, these two capillaries have larger outer diameters, so are more rigid and easier to keep straight. Even though these two fibers have lower fractional open area than fiber A, their transmissions exceeds that of fiber A at energies above 30 keV. The simulation also requires smaller waviness and bending correction for these two capillaries. Fiber E is thinner than type A, but its transmission is flat to 40 keV. The reason for this is that this fiber has small channel size which reduces the sensitivity to waviness and other profile errors. But the small channel size also results in more reflections being needed for a photon to traverse the fiber and may also have introduced other defects such as closed channels. This is why the transmission is only 40% under 40 keV although the open area is around 55%.

The high transmissions and the simulation results show that the quality of the capillaries is quite good. The surface roughness is between 0.5 to 0.8 nm, and bending curvature is above 110 meters for fibers C and D.

To simulate the more complex geometries of complete lenses, an extensive modeling program describing the propagation of x-rays along capillaries was developed by X-Ray Optical Systems, Inc. This provides essential information on the transmission efficiency and divergence of capillary optics. Some delay in the commencement of this task was created by the necessity of assuring the confidentiality of the proprietary code while providing access to student researchers. Access has been provided, and simulations of a collimating lens have been completed. It is essential to verify the simulation by comparison with measured data before the results of the design analysis of task I.D can be trusted. Analysis and comparison of the simulation to actual lens

THIS PAGE CONTAINS PROPRIETARY OR UNPUBLISHED DATA

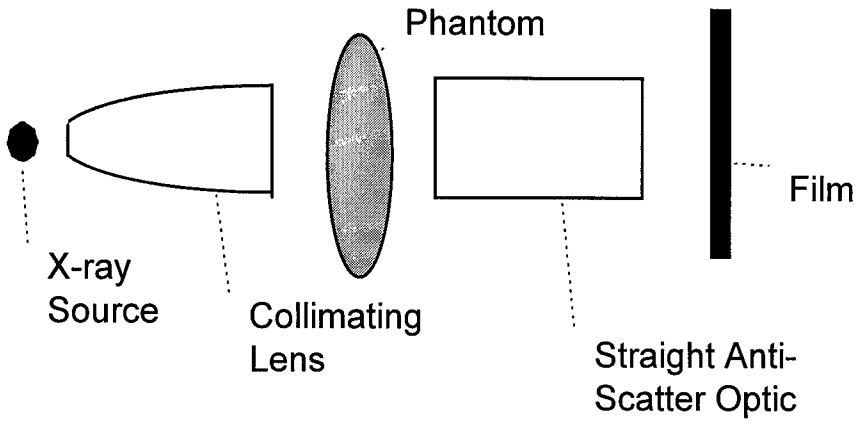

Figure 11. Set-up for Anti-scatter measurements.

measurements is reported in task IC.

Task I.C.

Assembly and Testing of Prototype Optic

Some difficulties have arisen in the production of high quality prototypes of large diameter. The combination of measurement and simulation described in task 1B has been beneficial in analyzing the manufacturing process. Small scale magnifying optics have been produced and tested, and additional small magnifying optics and demagnifying optics are expected to be available this quarter.

Because of the technological difficulties in producing curved monolithic optics, the fastest route to a large scale antiscatter system for contrast measurements is a straight optic. The low angular acceptance of the capillary channels requires that such an optic be used with a collimated beam as shown in Figure 11. A collimating lens and straight fiber bundle of 3 cm diameter have been obtained. A similar lens is pictured in Figure 13. The collimating lens was designed for 8 keV, but has a transmission of 14% at 20 keV. In addition to aligned transmission measurements, the variation in transmission as a function of entrance angle is important for estimating the scatter rejection properties of other full optics. This variation was measured by first aligning the source with the lens and then moving the source in the plane

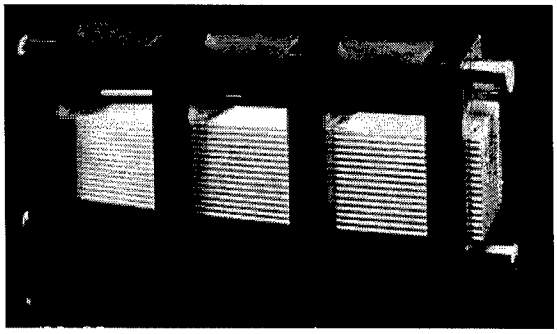

Figure 13. Multifiber collimating lens.

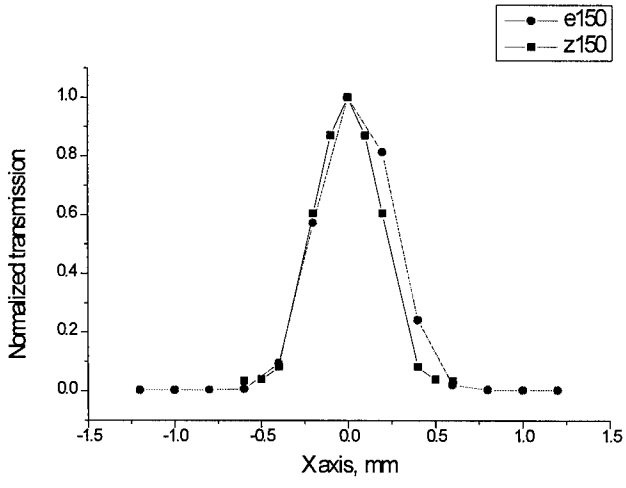

Figure 12. Transmission of a multifiber collimating lens as the source is moved transverse to the lens axis. Circles are measured data, and boxes simulation results.

THIS PAGE CONTAINS PROPRIETARY OR UNPUBLISHED DATA

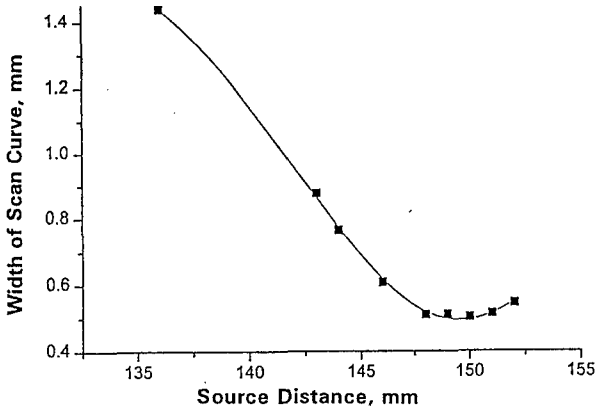

Figure 15. Width of scan of transverse source direction, as a function of source distance, for collimating lens, measured at 20 keV.

transverse to the capillary axis. The transmission efficiency decreases when the x-ray source is moved off-axis because the angle between the x ray and the reflection surface of the capillary increases. Because the reflectivity decreases sharply with angle this produces greater loss at each reflection. In addition x rays traveling through the capillary at a larger angle undergo more reflections. A comparison of measured and simulated data, with good agreement, is shown in Figure 12. Variation in the width of the scan as a function of the lens to source distance is the most reliable method of determining both the focal distance of the lens, and the depth of field. The measured variation is plotted in Figure 15. The depth of field can also be seen in Figure 14, which shows the measured and simulated transmission as a function of source to lens distance. The depth of field is about 11 mm.

Measurements of the exit divergence of the collimating optic have been performed at 8 keV and at 20 keV. Exit divergence is important if a capillary optic is to be used as a collector fore slit before the patient. In this case, the spatial resolution will depend on the angular spread of x-rays at the exit end of the capillaries. Large angular divergence is equivalent to a large focal spot size in a conventional system. The full width of the divergence measured at 20 keV is 2.56mrad, slightly greater than the critical angle for total external reflection.

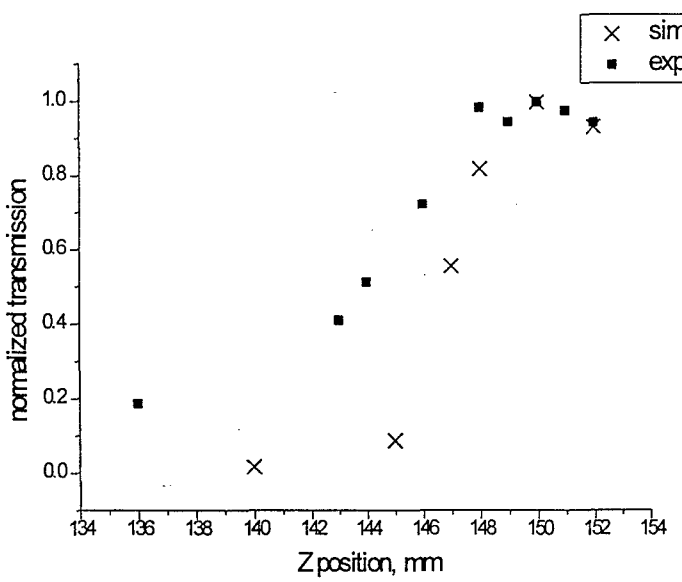

Figure 14. Variation in measured (box) and simulated (x) transmission as the source is moved towards the lens along the fiber axis.

Task I.D. Design of Final Mammographic Optics and Detector Unit

To overcome the manufacturing difficulty inherent in producing large diameter monolithic optics, the design decision has been made to concentrate on small scale prototypes

THIS PAGE CONTAINS PROPRIETARY OR UNPUBLISHED DATA

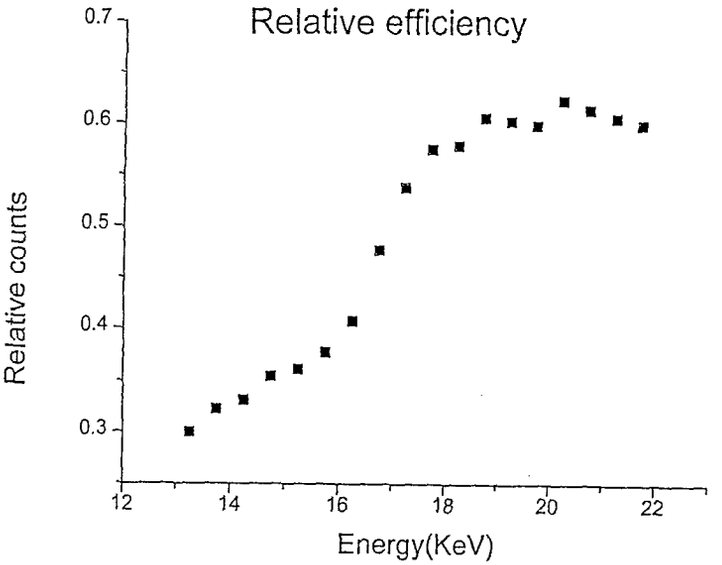

Figure 16. Detector quantum efficiency of CZT detector with thick aluminum windows.

which might be assembled into a large optic using a technique similar to that used to produce multifiber lenses.

Task II.A. Fabricate CZT Linear Detector Arrays

Digirad, Inc. (formerly Aurora Technologies) was somewhat delayed by the late start date of their subcontract with the University at Albany due to contract formalities. However, four 1 cm long CZT arrays with 50 μm pixels have been manufactured.

Task II.B. Develop Interconnect Methodology

The interconnect options were researched and the decision was reached to employ indium bump technology to bond the detector to a sapphire or quartz interconnect board, which is then bonded to the readout chips. This approach eliminates the need to wirebond to the detector, and also reduces the pixel size and consequently the leakage current. The first prototype has demonstrated some mechanical instability. It is believed this is fixable with epoxy, which will be attempted after the first round of electronic testing is complete.

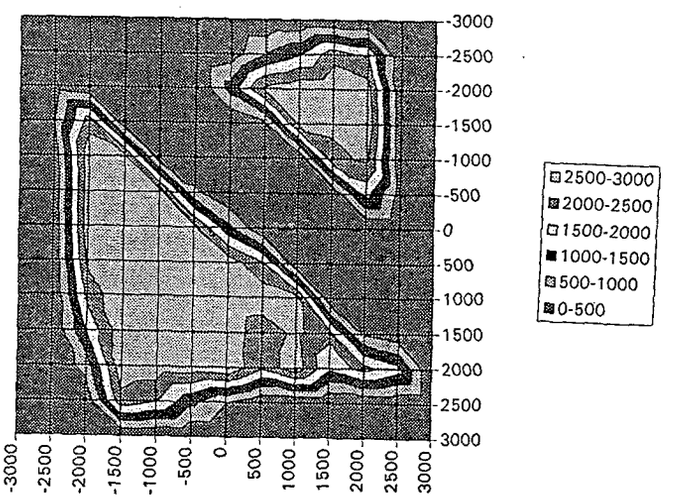

Figure 17. Scan of single pixel detector. Gray scale corresponds to measured sensitivity. x and y units are microns.

Task II.C. Assemble and Test Proof of Principle Detector/Multiplexer Hybrid

A CdZnTe array has been produced and bonded to the readout electronics for testing. Electronics for display readout have been designed, built and tested and were recently delivered to the University of Albany. In addition, a

single pixel element has been supplied to the University at Albany for characterization and determination of DQE. The DQE was measured in comparison with a high purity Ge detector (assumed to have DQE of unity in this energy regime). The result is shown in Figure 16 for the single pixel, which was fitted with a thick aluminum window. When the transmission of the window is taken into account, the DQE of the pixel is approximately one at 20 keV. The detector uniformity was measured by scanning a 300 μm pixel across the face and recording the scanned intensity. The result for the first single pixel detector is shown in Figure 17. A band of contact material obscured the face of the pixel. When this was removed, the detector scan was square and

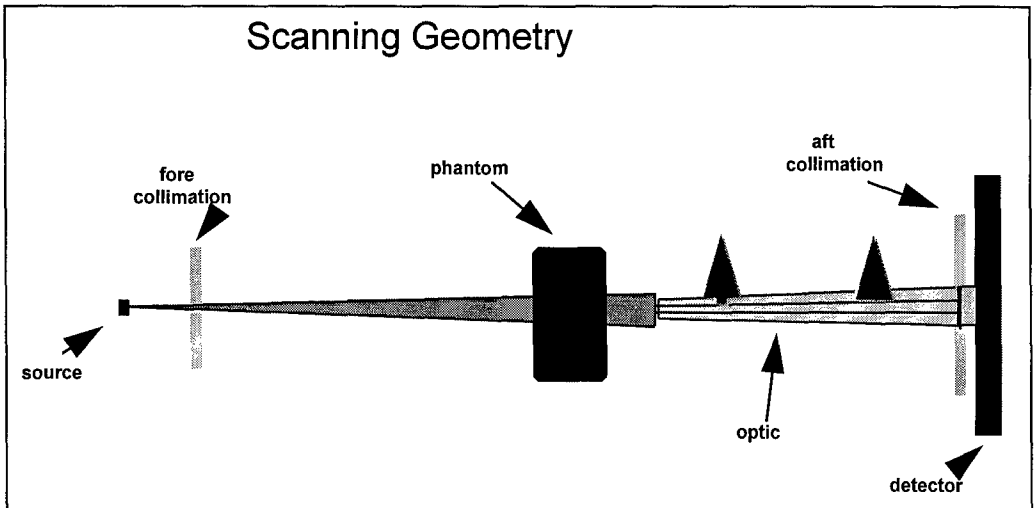

Figure 19. Small optic scanning geometry for contrast and imaging measurements.

uniform.

Task III.A. Measurement of Prototype System

Contrast enhancement measurements have been performed with a small scale

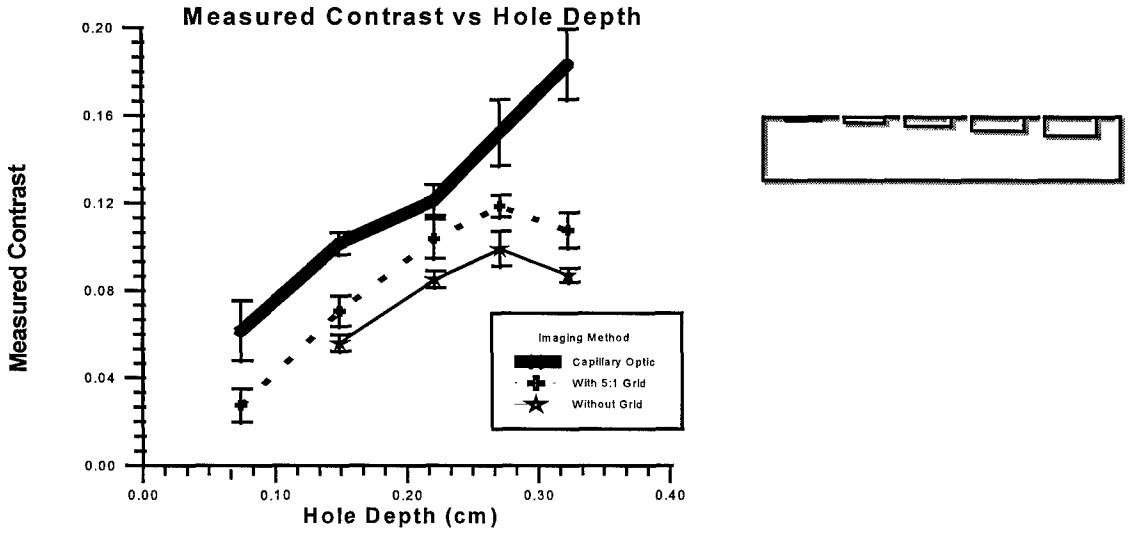

Figure 18. Contrast enhancement measured for a small scanned capillary optics using a phantom consisting of a Lucite block with drilled holes.

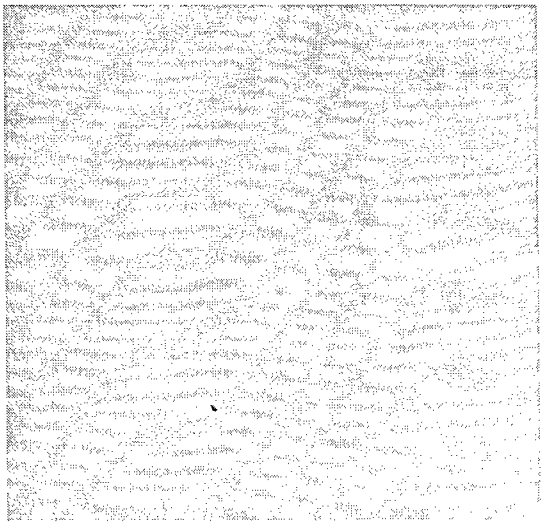

Figure 22. Image of contrast phantom produced with conventional grid.

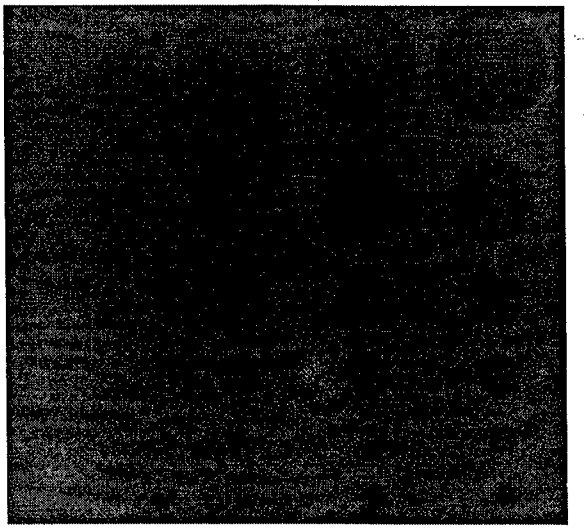

Figure 21. Image of contrast phantom produced with capillary optic.

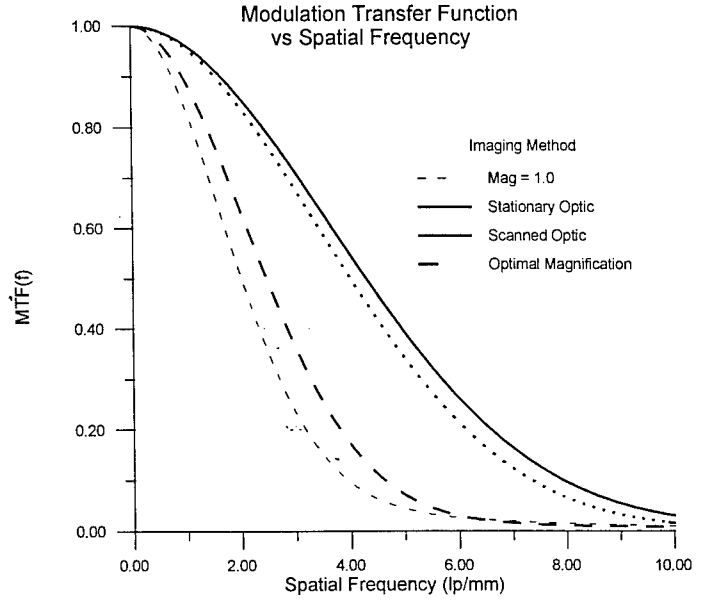

Figure 20. Modulation Transfer Frequency measurement with and without the optic.

(2 mm diameter) optic as part of an on-going collaboration with the Univ. of Wisconsin.[14] The geometry for the scan is shown in Figure 19, and the resulting contrast enhancement compared to the no optic and conventional grid cases are shown in Figure 18. Improvements have been made in the scanning system to reduce image artifacts. Scan lines which were visible in previous images are not apparent in Figure 21. The optic was also used to measure the resolution enhancement due to magnification. A plot of the measured MTF is shown in . At the 0.1 MTF level, the resolution improved from 4.5 lp/mm^2 without the optic to 8.9 lp/mm^2 with the optic.

Conclusions

Measurements have been performed of transmission and absorbence of single capillaries. Preliminary measurements have been performed of pre-prototype optics. These measurements indicate that capillary x-ray optics should be suitable for enhancing contrast and performing beam shaping for matching with digital detectors. Simulation work on a collimating optic has shown good agreement with data and is progressing, which has allowed some design decisions for a suitable optic to be made.

A prototype linear detector array has been constructed, along with readout electronics. A single pixel detector has been characterized.

References

[1] Shern, F., Digital Mammography and Related Technologies: A Perspective from the national Cancer Institute, Radiology, 183(3), p.629-630, 1992.

[2] M.A. Kumakhov, F.F. Komarov, "Multiple Reflection from Surface X-Ray Optics," Physics Reports, **191**, (5): p. 289-350, 1990.

[3] C.A. MacDonald, C.C. Abreu, S.S. Budkov, H. Chen, X. Fu, W.M. Gibson, Kardiawarman, A. Karnaukhov, V. Kovantsev, I. Ponomarev, B.K. Rath, J.B. Ullrich, M. Vartanian, Q.F. Xiao, "Quantitative Measurements of the Performance of Capillary X-Ray Optics," Multilayer and Grazing Incidence X-Ray/EUV Optics II, R.B. Hoover and A. Walker, eds., SPIE Proc. vol. 2011, 1993.

[4] J.B Ullrich, V. Kovantsev, C.A. MacDonald, "Measurements of Polycapillary X-Ray Optics," Jour. Appl. Phys., **74** (10), to be published, Nov. 15, 1993.

[5] C.A. MacDonald, "Applications and Measurements of Polycapillary X-Ray Optics," submitted, Journal of X-Ray Science and Technology, Special Issue for the Proceedings of the Monochromatic X-Ray Workshop, 11/93.

[6] C. C. Abreu, D. G. Kruger, C. A. MacDonald, C. A. Mistretta, W. W. Peppler, Q. F. Xiao, Measurements of Capillary X-Ray Optics with Potential for Use in Mammographic Imaging, accepted, Medical Physics.

[7] A. G. Haus, in **Screen Film Mammography**, G.T. Barnes and G. Donald Frey, eds., Medical Physics Publishing, Madison, Wisconsin, 1991.

[8] B.H. Hasegawa, The Physics of Medical X-Ray Imaging, 2nd Ed., Medical Physics Publishing, Madison, Wisconsin, 1991.

[9] Lei Wang and C.A. MacDonald, "Measurement of Capillary Optic Performance for Hard X rays," in R.B. Hoover and M.B. Williams, **X-Ray and Ultraviolet Sensors and Applications**, SPIE vol. 2519, July 1995.

[10] Lei Wang and C.A. MacDonald, "Measurement and analysis of capillary optic performance for hard x-rays", **Hard X-Ray/Gamma-Ray and Neutron Optics, Sensors, and Applications**, R.B. Hoover, and F.P. Doty, eds., SPIE Proceedings Vol. 2859.

[11] Q.F. Xiao, I.Y. Ponamarev, A.I. Kolomitsev and J.C. Kimball, in R.B. Hoover, ed., **X-Ray Detector Physics and Applications**, SPIE 1992.

[12] B.L. Henke, E.M. Gullikson, and J.C. Davis, Atomic Data and Nuclear Data Tables, **54 (2), p. 181, 1993.**

[13] Lei Wang, B.K. Rath, W.M. Gibson, J.C. Kimball, C.A. MacDonald, "Measurement and Analysis of Capillary Optic Performance for Hard X rays,", Jour. Appl. Phys., September 15, 1996.

[14] D.G. Kruger, C.C. Abreu, W.W. Peppler, C.A. MacDonald, C.A. Mistretta, "Imaging Characteristics of X-Ray Capillary Optics in Mammography," submitted, Medical Physics.

DEPARTMENT OF THE ARMY
US ARMY MEDICAL RESEARCH AND MATERIEL COMMAND
504 SCOTT STREET
FORT DETRICK, MARYLAND 21702-5012

REPLY TO
ATTENTION OF:

MCMR-RMI-S (70-1y) 1 JUN 2001

MEMORANDUM FOR Administrator, Defense Technical Information Center (DTIC-OCA), 8725 John J. Kingman Road, Fort Belvoir, VA 22060-6218

SUBJECT: Request Change in Distribution Statement

1. The U.S. Army Medical Research and Materiel Command has reexamined the need for the limitation assigned to technical reports. Request the limited distribution statement for reports on the enclosed list be changed to "Approved for public release; distribution unlimited." These reports should be released to the National Technical Information Service.

2. Point of contact for this request is Ms. Judy Pawlus at DSN 343-7322 or by e-mail at judy.pawlus@det.amedd.army.mil.

FOR THE COMMANDER:

Encl

PHYLLIS M. RINEHART
Deputy Chief of Staff for
Information Management

DAMD17-94-J-4413	ADB261602
DAMD17-96-1-6112	ADB233138
DAMD17-96-1-6112	ADB241664
DAMD17-96-1-6112	ADB259038
DAMD17-97-1-7084	ADB238008
DAMD17-97-1-7084	ADB251635
DAMD17-97-1-7084	ADB258430
DAMD17-98-1-8069	ADB259879
DAMD17-98-1-8069	ADB259953
DAMD17-97-C-7066	ADB242427
DAMD17-97-C-7066	ADB260252
DAMD17-97-1-7165	ADB249668
DAMD17-97-1-7165	ADB258879
DAMD17-97-1-7153	ADB248345
DAMD17-97-1-7153	ADB258834
DAMD17-96-1-6102	ADB240188
DAMD17-96-1-6102	ADB257406
DAMD17-97-1-7080	ADB240660
DAMD17-97-1-7080	ADB252910
DAMD17-96-1-6295	ADB249407
DAMD17-96-1-6295	ADB259330
DAMD17-96-1-6284	ADB240578
DAMD17-96-1-6284	ADB259036
DAMD17-97-1-7140	ADB251634
DAMD17-97-1-7140	ADB259959
DAMD17-96-1-6066	ADB235510
DAMD17-96-1-6029	ADB259877
DAMD17-96-1-6020	ADB244256
DAMD17-96-1-6023	ADB231769
DAMD17-94-J-4475	ADB258846
DAMD17-99-1-9048	ADB258562
DAMD17-99-1-9035	ADB261532
DAMD17-98-C-8029	ADB261408
DAMD17-97-1-7299	ADB258750
DAMD17-97-1-7060	ADB257715
DAMD17-97-1-7009	ADB252283
DAMD17-96-1-6152	ADB228766
DAMD17-96-1-6146	ADB253635
DAMD17-96-1-6098	ADB239338
DAMD17-94-J-4370	ADB235501
DAMD17-94-J-4360	ADB220023
DAMD17-94-J-4317	ADB222726
DAMD17-94-J-4055	ADB220035
DAMD17-94-J-4112	ADB222127
DAMD17-94-J-4391	ADB219964
DAMD17-94-J-4391	ADB233754